

FRESCO: Fast Radiometric Egocentric Screen Compensation

Matthew Post^{1,2} Paul Fieguth¹ Mohamed A. Naiel¹ Zohreh Azimifar³ Mark Lamm²

¹Vision and Image Processing Lab, University of Waterloo, Waterloo, ON, Canada

²Christie Digital Systems Canada Inc., Kitchener, ON, Canada

³Shiraz University, Shiraz, Iran

{mpost, pfieguth, mohamed.naiel, azimifar}@uwaterloo.ca, mark.lamm@christiedigital.com

Abstract

Existing radiometric compensation methods for projector-camera systems have been shown to produce compensated colours which are inconsistent to a human viewer. In this paper, a novel radiometric compensation method for projector-camera systems and textured surfaces is introduced based on the human visual system (HVS) colour response. The proposed method can extend established compensation methods to produce colours which are human-perceived to be correct (egocentric modelling). As a result, this method performs radiometric compensation which is not only consistent and precise, but also produces images which are visually accurate to an external colour reference. This method is shown to produce generally the lowest average radiometric compensation error when compared to compensation performed using only the response of a camera, demonstrated through quantitative analysis of compensated colours, and supported by qualitative results.

1. Introduction

The industry of projector displays extensively utilizes light projection on a wide variety of surfaces to paint a virtual canvas [1–4]. Projector displays have a wide range of applications including cinema displays, amusement rides, or to project video content onto arbitrary surfaces that can range from the flat sides of buildings, to cars, museum interiors, sports arenas, and abstract sculptures. When these surfaces have colourations or textures, the effect of image projection onto these surfaces is clearly influenced by the background texture [5]. Projector-camera systems [5, 6] are used to provide feedback to compensate and adjust the projected image to reduce or, ideally, eliminate the effects of the background.

Conventional projector radiometric compensation schemes [6–8] are limited by the colour sensitivity of the calibration camera, since the subjective balance of the cam-

era colour components determines the actual colours which are produced on-screen, resulting in compensation which appears incorrect to a human viewer. Thus, the addition of a mapping from camera tristimulus colour to human tristimulus colour will allow radiometric compensation to be performed with respect to the colour sensitivity of a human viewer rather than that of a camera. To the best of our knowledge, no method for radiometric compensation has been presented which can calibrate projector colours for a human viewer rather than that of a camera.

In this paper, a novel projector radiometric compensation method is proposed that utilizes a mapping between the spectral sensitivities of a camera and a human viewer. This method introduces the mapping of a camera colour response to human colour response using a projector stimulus for the first time. This radiometric compensation method is developed for linear systems and subsequently extended to nonlinear ones.

2. Related Work

The purpose of performing radiometric compensation with a projector-camera system is to provide perceived uniformity in images seen on the projection surface. This can be done either to compensate for non-uniformity of the projection surface [9] or of the light source itself [6]. This compensation is generally accomplished by using the camera in the system to determine the relationships between commanded projector intensities and colours observed on the surface.

Early methods for radiometric compensation were proposed using per-pixel linear solutions of increasing complexity [5, 7–9]. For instance, in [9] a method for compensating single-channel systems is introduced, which solves for a single gain value to be applied per-pixel in each target image, thereby compensating for the luminance but not compensating multiple colour channels simultaneously. Others proposed three-channel colour compensation [5, 7] by including colour mixing between projector and camera. These methods aim to produce colours to appear correct to a

camera by modeling the light contributions from each projector channel to each camera channel by use of a 3×3 matrix solution per pixel. Ambient light was incorporated into radiometric compensation methods through the introduction of an additional column to the compensation matrices [7]. Recently, several methods have been proposed for radiometric compensation of nonlinear systems [3, 6, 10]. For example, a method for making the solution for per-pixel nonlinear systems feasible has been introduced in [6], where a lookup table is used to provide the compensation for each pixel. Later in [10], a method was proposed for separating the nonlinearity of the system from the pixel-wise colour response to greatly reduce both the memory and computational requirements imposed by the nonlinear solution in [6]. These methods [6, 10] linearize a projector-camera system with a nonlinear response, but do not consider this for the nonlinearity or colour response of the human visual system.

Recent compensation methods [9, 11] have attempted to provide better compensation for viewers by modelling the human visual system. These methods improve visual quality of a scene by reducing edge artifacts from backgrounds in images, placing focus on contrast and edge sensitivity, but do not model human colour perception. For instance, the method outlined in [9] reduces edge artifacts due to background by dynamically scaling the intensity of a target image until the perceived edges are reduced in strength to below the threshold of human perception. However, this method does not perform radiometric correction to preset target colours, and instead aims to make the camera colour response equal to the colour of the target image while reducing luminance and contrast to reduce edge artifacts from the background. The effects of perception to colour were outlined in [12], where compensation of content is performed in a perceptually uniform space. This method does provide a means of adapting the compensation based on the content of the image, but does not account for the human perception of the projector colours.

The problem of luminance and colour non-uniformity was explored in [13], but the proposed solution did not maintain appropriate white balance in compensated images when the projector colour channels were solved independently and instead perform single-channel luminance balancing. Most of the existing radiometric compensation and screen colour correction techniques [4, 6, 14, 15] have optimized the compensated projector outputs to appear accurate to a white point of a camera, or used a previously colour-calibrated projector. All of the methods mentioned above have not yet been extended to include the human visual colour response, and thus can be improved by better modeling of the human visual system.

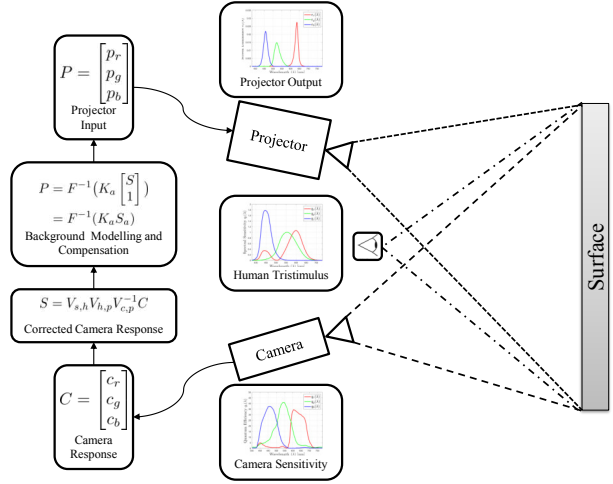


Figure 1: An overview of the proposed radiometric compensation scheme: Although a camera is used as feedback, the compensation scheme *explicitly* targets the human visual space, and not the camera space.

3. Proposed Method

Modelling the colour response of the human visual system provides an alternative to a camera as a sensing method for performing radiometric compensation. Figure 1 shows an overview of the proposed scheme, consisting of a projector, camera, human viewer, computer and a surface to be compensated. In the proposed method, the colour response of a camera is corrected to accurately represent the colours as seen by the human viewer. The human colour response is subsequently mapped to the colourspace of the desired projector content, allowing the radiometric compensation for a given background and projector to be performed with respect to the human eye, and not just to a camera. The proposed radiometric compensation scheme will be developed to determine an independent solution for each individual pixel on a given projection surface.

3.1. Representation of Spectral Responses

In this section, the relationships that govern the spectral responses for the human eye and a camera with respect to a projector stimulus are presented. The human colour response to light stimuli can be represented as a tristimulus model [16] consisting of three gain functions as seen in Figure 2.

Let the spectral output of a projector $e_j(\lambda)$ be defined as

$$e_j(\lambda) = P_j w_j(\lambda), \quad (1)$$

where $w_j(\lambda)$ is the light intensity output of the j th stimulus (such as a projector colour channel) as a function of wavelength λ , and P_j is the proportional gain corresponding to

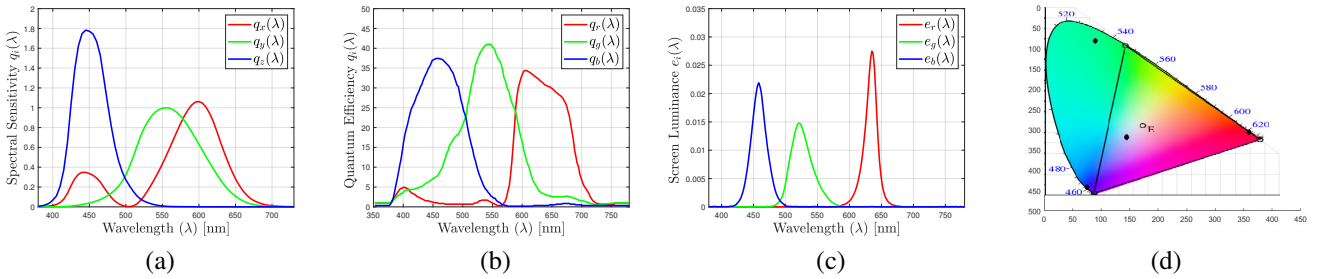


Figure 2: An illustration of example spectral responses for human tristimulus curves (a), camera tristimulus curves (b), and the spectral output of a Christie Matrix StIM LED projector (c). Further, (d) shows the projector primaries in xy colourspace obtained for (c) as seen by (a).

this j th stimulus. Next, let $q_i(\lambda)$ denote the response of the i th sensor (such as a camera colour channel or human retinal cell type) as a function of wavelength λ . It has been shown [5] that the resultant response, r_i , of the i th sensor to the combined reflected stimuli can be expressed as

$$r_i = \sum_j v_{i,j} P_j \quad (2)$$

where

$$v_{i,j} = \int_{\lambda_{\min}}^{\lambda_{\max}} q_i(\lambda) w_j(\lambda) s(\lambda) d\lambda. \quad (3)$$

Here $s(\lambda)$ is the surface reflectance for a given light wavelength, and λ_{\min} and λ_{\max} are the bounds of the sensor wavelength sensitivity. Examples of the response curves $q_i(\lambda)$ and projector stimuli $e_j(\lambda)$ can be seen in Figure 2 (a-c). It must be pointed out that both the camera response (quantum efficiency) and projector stimuli (spectral output) are highly dependent on the characteristics of the respective devices.

As derived in (3) the sensor tristimulus colour response, $v_{i,j}$, is represented by the inner product of three colour sensitivity functions $q_i(\lambda)$ of a given camera or human colour perception model (such as CIE 1931 [16] and CIE 1964 [17]) and the spectral outputs of each projector channel $w_j(\lambda)$ with a given screen spectral reflectance $s(\lambda)$. The projector spectral output $w_j(\lambda)$ can not be measured directly, however, from (1) it follows that

$$w_j(\lambda) \propto e_j(\lambda) \quad (4)$$

where $e_j(\lambda)$ can be approximated by the measurements of a spectroradiometer. The projector spectra only need to be measured once and stored for each projector type, which removes the requirement of measuring the spectrum at the time of radiometric compensation.

Let C and H be the spectral responses of the camera sensor and human visual system, respectively, and let P be the channelwise input to the projector. For instance, these vectors can be expressed in terms of three primary channels,

RGB or XYZ, as

$$C = \begin{bmatrix} c_r \\ c_g \\ c_b \end{bmatrix}, \quad H = \begin{bmatrix} h_x \\ h_y \\ h_z \end{bmatrix}, \quad P = \begin{bmatrix} p_r \\ p_g \\ p_b \end{bmatrix} \quad (5)$$

where the subscripts r, g, b denote the three channels of an RGB colour model, and x, y , and z denote the three channels of an XYZ colour model. Let $V_{c,p}$ and $V_{h,p}$ be of size (3×3) that denote the projector colour mixing matrices for the camera and human visual system, respectively. By substituting in (3) these matrices can be expressed as follows:

$$V_{c,p} = \begin{bmatrix} v_{rr} & v_{rg} & v_{rb} \\ v_{gr} & v_{gg} & v_{gb} \\ v_{br} & v_{bg} & v_{bb} \end{bmatrix}, \quad V_{h,p} = \begin{bmatrix} v_{xr} & v_{xg} & v_{xb} \\ v_{yr} & v_{yg} & v_{yb} \\ v_{zr} & v_{zg} & v_{zb} \end{bmatrix} \quad (6)$$

From (2), the response of a camera to a projector, as well that of a human visual system to a projector, can be represented as

$$C = V_{c,p} P \quad (7)$$

$$H = V_{h,p} P \quad (8)$$

Existing state-of-the-art radiometric compensation methods, such as [5–7], correct for colours as seen by the calibration camera by modelling the inverse of (7), and do not compensate for the colours seen by a human viewer. Although these compensation techniques provide reasonably precise correction of screen uniformity, they cannot accurately calibrate to an exact desired colour. From Figure 2 (d), human responses to the projector primaries and white are different from the target colours as seen when calibrated to a camera’s response. This difference in colour calibration result is due to the differences in the shape of the human and camera sensor response curves used in (3); as a result

$$V_{c,p} \neq V_{h,p}. \quad (9)$$

Thus, it is evident that a mapping between the human and camera responses is required. In the following section, a mapping from camera spectral response to a model of a human spectral response using the stimulus of a projector is introduced.

3.2. Mapping of Spectral Responses

To map a given camera colour response to a human colour response, the sensitivity of both sensors to a given projector stimulus are first determined by (7) and (8). This portion of the calibration needs to be performed only once for a given projector-camera pair. The projector spectrum is used as an intermediary reference point to establish the relationship between camera and human colour responses. This relationship will then be used to eliminate any system dependency on camera pre-calibration or *a priori* knowledge of the quantum efficiency of the camera.

The mapping between camera and human responses can be determined by substituting P from (7) into (8) as follows:

$$H = V_{h,p}V_{c,p}^{-1}C. \quad (10)$$

To perform radiometric compensation in the colour space of content images, the human colour response H can be mapped to a colour S of size (3×1) in a standard colourspace (such as an RGB space with linear gamma) by using a known mapping, $V_{s,h}$ [18]:

$$S = V_{s,h}H \quad (11)$$

From (10) and (11), a mapping of the camera response into a standard colourspace can now be determined as

$$S = V_{s,h}V_{h,p}V_{c,p}^{-1}C \quad (12)$$

By transforming the colours as seen by the camera C to a camera invariant colourspace, the radiometric compensation can be performed using S , which will be referred to as the *corrected camera response*.

3.3. Compensation in Mapped Space

In this section, the relationship in (12) will be utilized in order to perform radiometric compensation with a camera response corrected with respect to a human viewer. This radiometric compensation will be established first for linear projector systems without ambient light. Then, to consider practical projector situations, the proposed method will be extended to systems demonstrating nonlinear projector responses and operating in the context of ambient light contributions.

Background Modeling: From (7), the projector intensity P for a linear system can be represented as

$$P = V_{c,p}^{-1}C. \quad (13)$$

In order to map the camera response to the standard colourspace, both sides of (13) are multiplied by $V_{s,h}V_{h,p}$:

$$V_{s,h}V_{h,p}P = V_{s,h}V_{h,p}V_{c,p}^{-1}C. \quad (14)$$

Due to the effect of the background, the right-hand side of (14) can be approximated by S (12), so that the projector

intensity P that compensates for a given background can be simplified as

$$V_{s,h}V_{h,p}P \approx S \quad (15)$$

$$P \approx V_{h,p}^{-1}V_{s,h}^{-1}S \quad (16)$$

$$P \approx KS \quad (17)$$

where $K = V_{h,p}^{-1}V_{s,h}^{-1}$ is of size (3×3) and represents the matrix which compensates P given a projection background and corrected camera response S .

In the case where the projector is not the sole contribution to a sensor response, as in [19], the additional light contribution can be modelled by modifying K and S as follows:

$$P = \begin{bmatrix} K & | & k_{ra} \\ & | & k_{ga} \\ & | & k_{ba} \end{bmatrix} \begin{bmatrix} S \\ -- \\ 1 \end{bmatrix} \quad (18)$$

$$\equiv K_a S_a \quad (19)$$

Similar to [6, 10], the expression in (19) can be extended to the case of a nonlinear relationship between a projector and sensor response as

$$P = F^{-1}(K_a S_a) \quad (20)$$

where $F^{-1}(\cdot)$ is a function representing the inverse nonlinearity of the system that can be determined empirically by exhaustively sampling the domain of the projector gamut, and then stored as a lookup table for much faster computation.

In order to model the background, given P and the corresponding S_a for a series of test colours, the matrix K_a can be obtained as the least-squares solution of (19) or (20) for the linear or nonlinear case, respectively.

Background Compensation: In the compensation phase, since the pixel colours of a given input image are provided as the target colours to be seen on the screen and they are in the standard colourspace of S , these values are used as S to construct S_a . Next, the solved matrices K_a and S_a are used to directly compute the required projector output P for the linear or nonlinear case by using the relationship in (19) or (20), respectively.

4. Experimental Results

For projector calibration, eight flat-field test patterns are used: white, black, three primaries (red, green, blue), and three secondaries (cyan, yellow, magenta). The use of additional colours, beyond the commonly-used three primary and black colours, leads to greater stability of the solution for each pixel. The camera captures of each of these flat fields and the projected colours are then remapped using the matrix from (20) to determine the least-squares solution to K_a , where an RGB colourspace with linear gamma was chosen for the camera output.

4.1. Qualitative Results

Several backgrounds and target images have been selected to test the capabilities of the proposed radiometric compensation method under several challenging conditions. In particular, the proposed radiometric compensation scheme is evaluated by using three challenging background surfaces, namely *Brick*, *Rainbow*, *Textured Rainbow*, and the compensation is applied to nine different target images, namely, *Astronaut*, *Car*, *Cubes*, *Flower*, *Balloons*, *Skating*, *Plate*, *Yellowstone* and *Waterfall*. The first and second columns of Figure 3 show the test backgrounds and the target images, respectively. The *Brick* background represents the scenario of projection onto brick buildings, which is very challenging, particularly when compensating for the dark borders around bricks. The *Rainbow* and *Textured Rainbow* backgrounds both include a full range of colours, with *Rainbow* designed to have a range of extreme but smooth colour patches, whereas *Textured Rainbow* also requires compensation for higher frequency texture patterns in addition to the variations in chroma.

Figure 3 also demonstrates sample projector outputs and compensated results for the proposed scheme, and the captured results for projection without radiometric compensation and projection with radiometric compensation but without HVS. The first row of Figure 3 shows the results of projecting the *Astronaut* target image on *Brick* background. It is clear that the proposed scheme can provide compensation quality better than that of projection without using HVS, as the proposed scheme compensates to the correct colours and has reduced the effect of edges in the final image. In the second and third rows, the *Car* and *Cubes* target images have been projected; the proposed scheme offers colour uniformity, non-noticeable background edges, and maintains visual quality for the human viewer.

The middle three rows of Figure 3 show the results of projecting *Flower*, *Balloons* and *Skating* images on the *Rainbow* background. Unlike the method of projection without HVS, the proposed method provides not only highly uniform compensated images, but also shows accurate colours that are very close to the content colours. This also confirms the ability of the proposed scheme to solve for highly colourful background and content scenarios, and for the capability of projecting a sample sports content on a challenging background.

Finally, the last three rows of Figure 3 illustrate the results of projecting *Plate*, *Yellowstone* and *Waterfall* content images on the *Textured Rainbow* background. These results demonstrate the ability of the proposed method to produce compensated colours that are closer to the target colours of an image, rather than that of compensation without using HVS. This performance is consistent across the various textures, colours and environmental conditions.

4.2. Quantitative Results

For purposes of practical evaluation, two different projector classes¹ are used to assess the uniformity and accuracy of the compensation. The camera used in the system is a 5MP camera², which is used to provide feedback to the system for compensation. The projector models differ in their light sources, and include an LED based projector of linear colour response and a mercury lamp based projector of nonlinear colour response. The *Rainbow* background pattern shown in Figure 3 is used to provide a challenging background with uniformly coloured patches for which the compensation accuracy is measured by a spectroradiometer. This test background is designed with twelve different background colours, and each colour either being a primary, secondary, or tertiary colour in the RGB and CYM colour systems to challenge the limits of the compensation methods. For each compensation method, a spectroradiometer³ outside of the calibration loop is used to measure the screen compensation for four target colours on the coloured background patches. Each background patch provides a different uniform region upon which to position the circular measurement area of the spectroradiometer as seen in Figure 4, where the spectroradiometer measures the incident light from a 5 degree cone.

Measurements of xy and Luminance: From Figure 5, it can be seen that the proposed method significantly improves the white point in the resulting compensated images. The proposed method accurately compensates different projectors to the same reference white as seen by a human viewer, resulting in colours on screen which are perceptually consistent with a given target image. In addition, by compensating the projector to the correct white, the resulting compensation is more uniform overall for white, indicating not only greater fidelity for white images is achieved, but also the final image on screen is more uniform overall. Figure 5 also shows a fundamental limit of this method. This method can be used to accurately set the white point for compensation, but the chroma of the compensated primary colours remains anchored near the original values. Despite this, as shown in Figure 3 the proposed method is shown qualitatively to compensate for extremely adverse surfaces with minimal edge artifacts incurred from the backgrounds.

The last four columns of Figure 5 show the luminance required to create flat colour fields of white, red, green and blue that appear uniform using this method. As seen in this figure, the luminance drop is comparable to compensation without HVS mapping, and the flatness of these curves demonstrates the luminance uniformity of the image.

¹The projectors used were Christie Matrix StiM (LED) and Christie DWX600-G (Mercury Lamp).

²The PointGrey Flea3 Camera with GigE was used.

³This test was carried out using the JETI Specbos 1211.

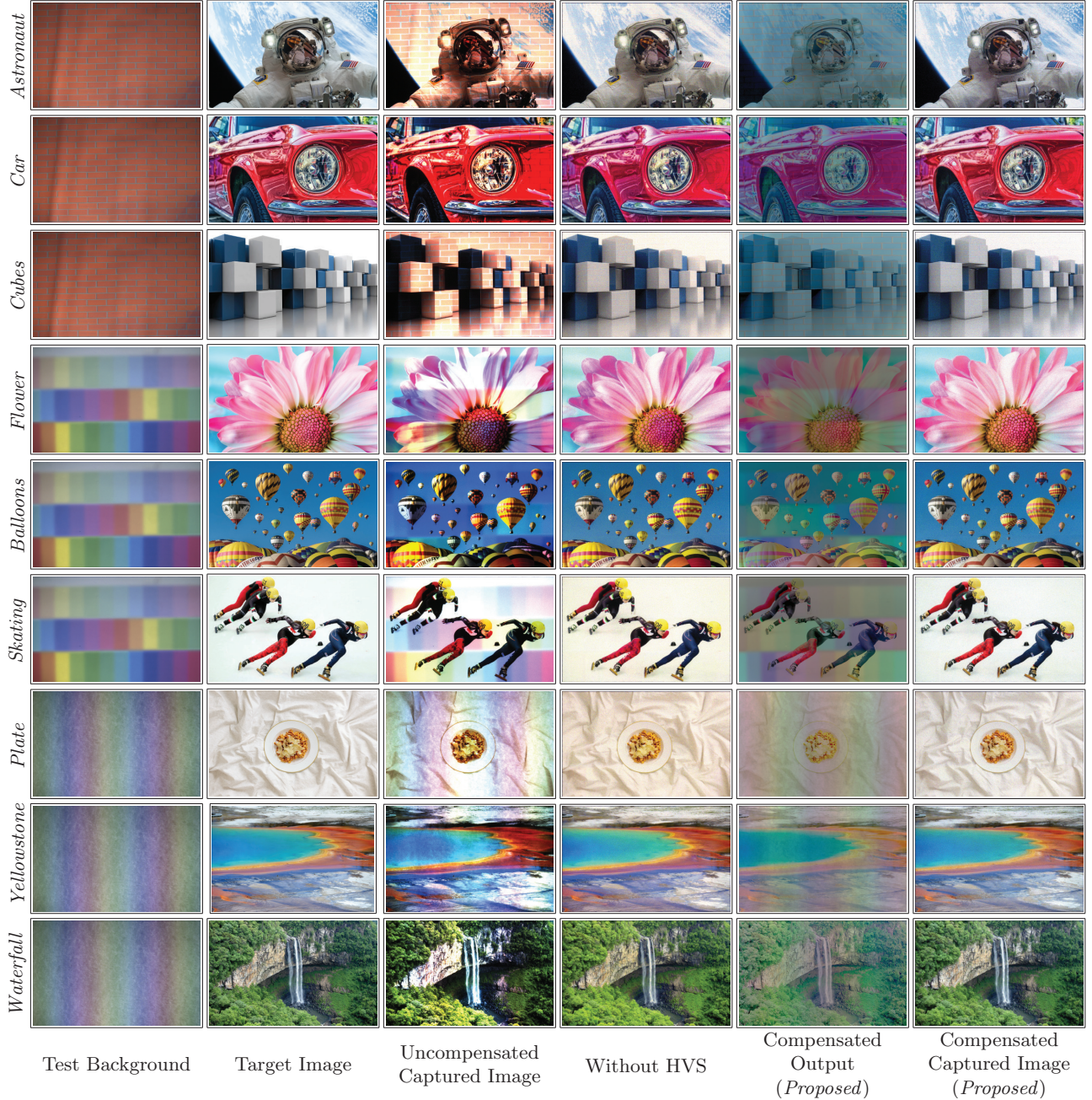


Figure 3: Sample qualitative results for the proposed scheme, uncompensated projection, and compensation without HVS correction on *Brick* (1st, 2nd and 3rd rows), *Rainbow* (4th, 5th and 6th rows) and *Textured Rainbow* (7th, 8th and 9th rows) backgrounds using nine different test images. All images are shown in projector coordinates.

This difference in luminance is exactly proportional to the amount of light the most troublesome regions of the image are capable of reflecting, as the entire compensated image must be reduced to have the same colour and luminance of the least reflective (darkest) portions of a background. Similar to radiometric compensation without human colour mapping, the proposed method cannot increase the light

output capabilities of a projector, but instead it must reduce the amount of light on screen to produce perceptually uniform images as seen in Figure 5.

Compensation Error: In order to evaluate the error between a target colour and the compensation measurements of a given method, the CIE ΔE [18] is used. This metric

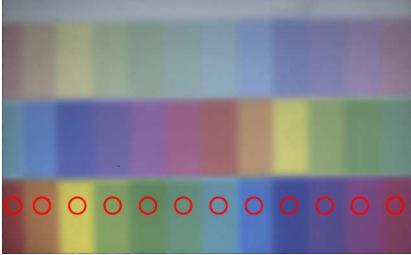


Figure 4: Illustration for the twelve different sample locations on the *Rainbow* background used for the spectroradiometer measurements.

is used to compute colour distance between a colour seen on screen and the desired target colour. The target colour provides only a chroma target for the compensation, and the luminance is dependent on the output capabilities of the projector in the system, thus the luminance component of the ΔE must be determined separately. For this investigation, the desired luminance is taken to be the average luminance of all screen patches, as deviation from this luminance indicates non-uniformity of the compensated image. In this way, the distance to both target chroma and the overall screen luminance are combined into a single error metric to quantify both accuracy and consistency of the compensated projector output.

Table 1 shows a comparison of the mean and standard deviation of the ΔE values obtained for the proposed method, performing radiometric compensation projection without HVS, and projection without compensation. As in the previous experiment, white, red, green and blue are used as the target colours using the same two types of projectors. As shown in this table, the proposed method offers the lowest average ΔE compared to that of radiometric compensation without HVS in six out of eight test cases, while maintaining nearly the same performance as non-HVS compensation in the remaining two cases.

Computational Cost: The storage requirements and computational time of the proposed method are verified through a Matlab implementation of the proposed method⁴, and then compared to that of the existing nonlinear method in [6]. The memory and computation times for nonlinear projector systems are assessed for three different common projector resolutions (720p, 1080p and 4K). As shown in Table 2, the proposed method uses less than $\frac{1}{5}$ of the memory and is $13 \times$ faster in compensation time than that of the method in [6], while maintaining the same computational complexity of radiometric compensation without HVS. The proposed scheme requires only a modest increase in time (less than 1 second per 4K image) during the image capturing portion of the background modelling phase than that of the baseline, due to correcting the captured camera colours (12).

⁴A CPU with 4 cores operating at 3.40GHz was used.

5. Conclusions and Future Work

In this paper, a new radiometric compensation method has been proposed for projector-camera systems and textured surfaces based on the colour sensitivities of a human viewer. This method introduces a mapping between camera and human colour perceptions through the use of a projector light source. It has been shown that by properly modelling the colour response of a human viewer, this method can produce approximately the same colours on a surface using different light sources and cameras. This eliminates the need for cameras and projectors which are previously radiometrically calibrated, with camera colour mappings instead being determined from the known spectral output of a projector. Experimental results have shown that the proposed method with using HVS generally offers the lowest average radiometric compensation error and closer to the target colours than that of compensation without HVS.

The direct consequence of this method is the ability to calibrate and match camera colour responses to others, or alternatively colour match two projectors without the need to be seen by the same camera. Further work is planned to investigate the impact of this method in performing colour calibration of blended screen multi-projector displays. Extending the proposed colour correction with respect to a human viewer to other nonlinear radiometric compensation methods is also a potential extension to this work.

6. Acknowledgment

We would like to thank the Ontario Centres of Excellence (OCE-VIP II), the Natural Sciences and Engineering Research Council of Canada (NSERC-CRD) and Christie Digital Systems for sponsoring this research work. This work is the intellectual property of Christie Digital Systems USA Inc.

References

- [1] B. Masia, G. Wetzstein, P. Didyk, and D. Gutierrez, “A survey on computational displays: Pushing the boundaries of optics, computation, and perception,” *Computers & Graphics*, vol. 37, no. 8, pp. 1012 – 1038, 2013.
- [2] M. Brown, A. Majumder, and R. Yang, “Camera-based calibration techniques for seamless multiprojector displays,” *IEEE Trans. on VCG*, vol. 11, no. 2, pp. 193–206, 2005.
- [3] S. Liu, “The color calibration across multi-projector display,” *J. of Signal Inf. Process.*, vol. 02, pp. 53–58, 2011.
- [4] J. Tsukamoto, D. Iwai, and K. Kashima, “Radiometric compensation for cooperative distributed multi-projection system through 2-DOF distributed control,” *IEEE Trans. on VCG*, pp. 1221–1229, 2015.
- [5] S. K. Nayar, H. Peri, M. D. Grossberg, and P. N. Belhumeur, “A projection system with radiometric compensation for screen imperfections,” in *Columbia University Technical Report*, 2003.

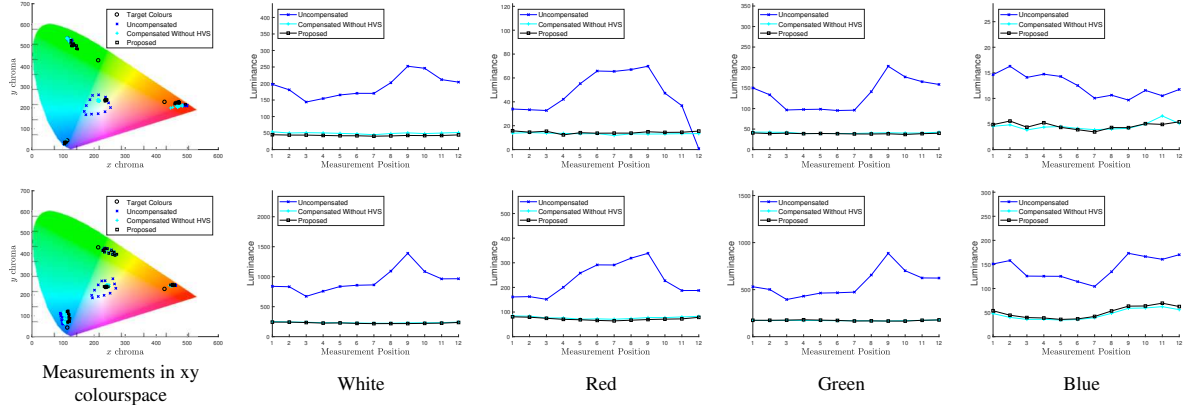


Figure 5: Comparing the measurements of the proposed method in the xy colourspace before and after compensation with and without using HVS, and the corresponding luminance plotted for each target colour, where a Christie Matrix StIM (LED) and DWX600-G (Mercury Lamp) projectors are used in the 1st and 2nd rows, respectively. In this figure, greater uniformity is indicated by a tighter points cluster in the xy colour chart or a flatter line in the luminance plots.

Table 1: Comparing means and standard deviations of ΔE for uncompensated projection, compensated projection but without using HVS and the proposed method, where the ΔE values are calculated for twelve patches when targeting four different colours. The ΔE [18] is a function representing the colour distance between the spectrometer measurement of a given patch and the given target colour. Note: boldface and underscore denote the best and second best results, respectively.

Methods	Christie Matrix StIM (LED) Projector				Christie DWX600-G (Mercury Lamp) Projector			
	White	Red	Green	Blue	White	Red	Green	Blue
Uncompensated	64.68 ± 29.00	86.12 ± 40.93	149.10 ± 52.1	66.53 ± 27.45	78.24 ± 26.91	68.08 ± 23.74	68.02 ± 35.00	265.37 ± 112.51
Comp. without HVS	16.52 ± 5.28	23.32 ± 10.43	80.05 ± 26.36	32.68 ± 12.60	13.78 ± 5.18	30.81 ± 9.89	40.98 ± 23.01	184.62 ± 71.02
<i>Proposed Method</i>	2.40 ± 1.38	10.56 ± 7.64	68.28 ± 21.91	32.32 ± 4.97	5.42 ± 2.97	31.23 ± 10.20	41.56 ± 23.22	122.98 ± 56.10

Table 2: Comparison of the memory and the time complexities of the proposed scheme with and without using HVS mapping, and that of the method in [6] at three different resolutions. Note: boldface denotes the best results and * denotes a calculated value.

Methods	Memory (GiB)			Time, CPU (s)		
	720p	1080p	4K	720p	1080p	4K
Grundhfer & Iwai [6]	2.50*	-	-	7.1	-	-
Comp. without HVS	0.46	0.56	1.17	0.53	0.82	2.10
<i>Proposed Method</i>	0.46	0.56	1.17	0.53	0.82	2.10

- [6] A. Grundhfer and D. Iwai, “Robust, error-tolerant photometric projector compensation,” *IEEE Trans. on Image Process.*, vol. 24, no. 12, pp. 5086–5099, 2015.
- [7] T. Yoshida, C. Horii, and K. Sato, “A virtual color reconstruction system for real heritage with light projection,” in *Proc. Int. Conf. on VSMM*, 2003, pp. 1–7.
- [8] O. Bimber, D. Iwai, G. Wetzstein, and A. Grundhoefer, “The visual computing of projector-camera systems,” *Computer Graphics Forum*, vol. 27, no. 8, pp. 2219–2245, 2008.
- [9] D. Wang, I. Sato, T. Okabe, and Y. Sato, “Radiometric compensation in a projector-camera system based properties of human vision system,” in *Proc. IEEE CVPR Workshops*, 2005, pp. 70–70.
- [10] M. Post, P. Fieguth, M. A. Nael, Z. Azimifar, and M. Lamm, “Fast radiometric compensation for nonlinear projectors,” in *Proc. Conf. Vis. and Intell. Syst. (CVIS)*, 2018, pp. 1–3.
- [11] T. Huang, C. Kao, and H. H. Chen, “Quality enhancement of

- procam system by radiometric compensation,” in *IEEE Int. Workshop on MMSP*, 2012, pp. 192–197.
- [12] M. Ashdown, T. Okabe, I. Sato, and Y. Sato, “Robust content-dependent photometric projector compensation,” in *Proc. IEEE CVPR Workshops*, 2006, pp. 1–6.
- [13] A. Majumder and R. Stevens, “Color nonuniformity in projection-based displays: analysis and solutions,” *IEEE Trans. on VCG*, vol. 10, no. 2, pp. 177–188, 2004.
- [14] A. Majumder, C. Browne, and M. S. Brown, *Practical multi-projector display design*. AK Peters/CRC Press, 2007.
- [15] Q. Jia, H. Xu, J. Song, and X. Gao, “Research of color correction algorithm for multi-projector screen based on projector-camera system,” in *Proc. ISDEA*, 2012, pp. 1285–1288.
- [16] D. B. Judd, “Extension of the standard visibility function to intervals of one millimicron by third-difference osculatory interpolation,” *J. Opt. Soc. Am.*, vol. 21, no. 5, pp. 267–275, May 1931.
- [17] I. Nimeroff, J. R. Rosenblatt, and M. C. Dannemiller, “Variability of spectral tristimulus values,” *J. Opt. Soc. of Am.*, vol. 52, 06 1962.
- [18] G. Sharma, W. Wu, and E. N. Dalal, “The CIEDE2000 color-difference formula: Implementation notes, supplementary test data, and mathematical observations,” *Color Research & Application*, vol. 30, no. 1, pp. 21–30.
- [19] S. Mihara, D. Iwai, and K. Sato, “Artifact reduction in radiometric compensation of projector-camera systems for steep reflectance variations,” *IEEE Trans. on CSVT*, vol. 24, no. 9, pp. 1631–1638, 2014.